Basic Orthopaedic Biomechanics, 2nd ed.,
edited by Van C. Mow and Wilson C. Hayes.
Lippincott-Raven Publishers, Philadelphia © 1997.

10

Biomechanics of the Human Spine

James A. Ashton-Miller and Albert B. Schultz

Biomechanics Research Laboratory, Department of Mechanical Engineering and Applied Mechanics, University of Michigan, Ann Arbor, Michigan 48109-2125

Spine disorders are the most prevalent cause of chronic disability in persons less than 45 years of age and are second only to natural childbirth in accounting for hospital stays of patients under age 65 (183,209). In 1983, over 250,000 surgeries were performed on the spine in the United States (218). Although a small proportion of these concern the correction of congenital and idiopathic spine deformities, most relate to low-back and cervical spine disorders. The annual prevalence of low-back disorders in the U.S. population is about 15% to 20%; at any given time, back problems temporarily disable about 1% and chronically disable a further 1% of the population (10). In 1992, the annual costs associated with back pain in the United States ranged from $20 to $50 billion (179). Although the cause of most low-back disorders remains unknown, there is a clear association between strenuous work and lifting and the frequency and severity of spine disorders (9,77,146,171). For example, workers performing frequent heavy lifts from twisted positions have six times the risk of an acute lumbar disk prolapse of those who perform lighter work (128). These statistics and others confirming an association between heavy work and low-back disorders justify studies of the biomechanics of the human spine. However, it should also be noted that a large prospective study demonstrated that nonphysical factors such as job satisfaction and psychological attributes were also found to be important outcome predictors (38,39). A discussion of the range of treatment options that are available (40) is beyond the scope of this chapter.

This chapter reviews present knowledge of the basic biomechanics of the spine, empha-

sizing experimental measurements and techniques of biomechanical model analysis.

COMPONENTS OF THE TRUNK MUSCULOSKELETAL SYSTEM AND THEIR MECHANICAL PROPERTIES

The trunk musculoskeletal system consists of the spine, rib cage, and pelvis as well as associated fascia and musculature. The spine itself consists of 24 semirigid presacral vertebrae that are separated by relatively flexible intervertebral disks. Together with seven intervertebral ligaments that span each set of adjacent vertebrae, two synovial joints on each vertebra, called the zygapophyseal or facet joints, act to constrain relative motion.

The spine is divided into four regions: cervical, thoracic, lumbar, and sacral (Fig. 1). The thoracic spine serves as an integral part of the rib cage. Twelve pairs of ribs articulate posteri-

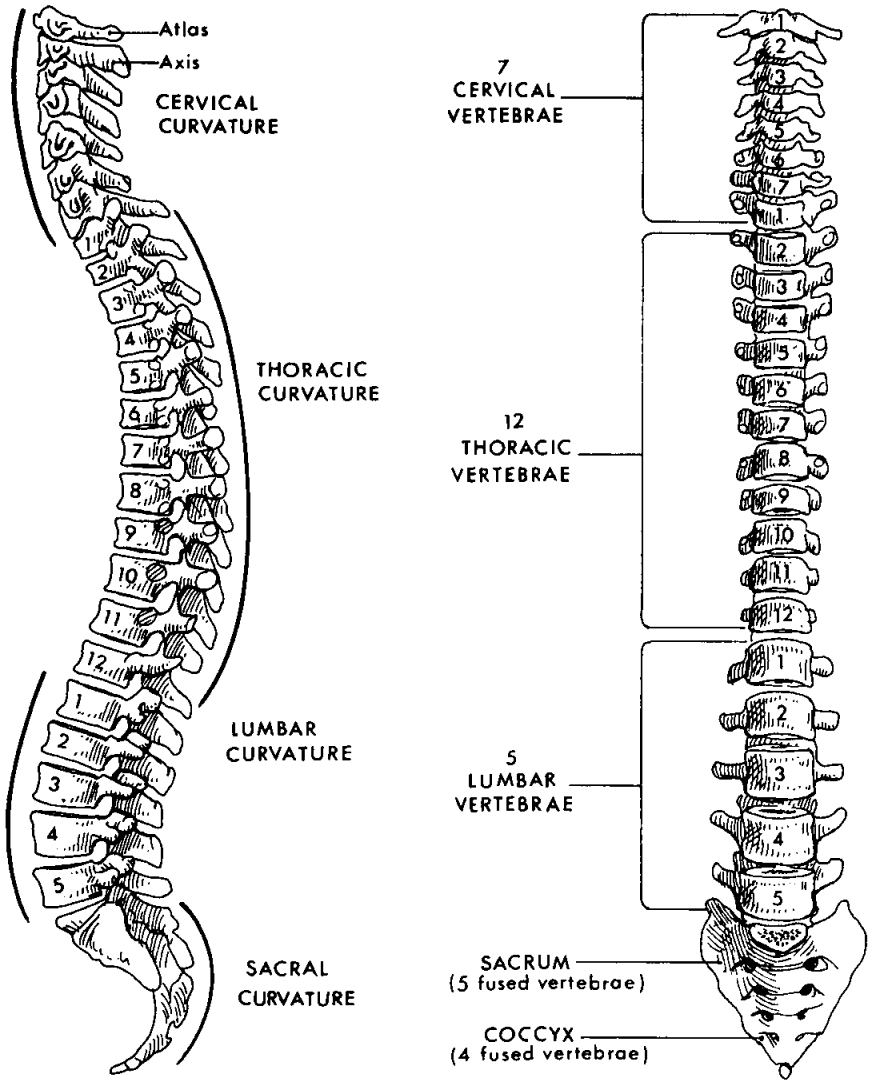

FIG. 1. Frontal *(right)* and left lateral *(left)* views of the human spine.

orly with the spine at the costovertebral joints; the upper ten pairs of ribs also articulate anteriorly with the sternum at the costosternal articulations. Movements of the rib cage relative to the thoracic spine occur during respiration, especially during strenuous activity. The sacral–coccygeal region is formed by nine vertebrae fused into a single bony mass that articulates with the right and left ilia (or innominate bones) to form the pelvis. The ilia articulate with the sacrum at the sacroiliac joints and with each other at the pubic symphysis. Enlargement of the birth canal at childbirth is the only time that appreciable movement of one ilium, relative to the other, normally occurs.

Bones and Joints

Vertebrae

With the exception of the upper cervical vertebrae, C-1 and C-2 (also known as the atlas and axis), each vertebra consists of an anterior structure known as the vertebral centrum and a complex configuration of posterior and lateral structures (note the lumbar vertebrae example, Fig. 2). This configuration is comprised of the structurally significant neural arch, made up of the pedicles and laminae that complete the spinal canal and the spinous and transverse processes, which serve primarily as muscle attachment sites. Each vertebra also has right and left superior and inferior articular processes, which in adjoining pairs constitute the right and left facet joints.

The vertebral centrum consists of trabecular bone surrounded by a thin cortical shell with an average thickness of 0.35 mm (244a). The centrum primarily resists compression and shear loading. Studies have shown that compression is carried mainly by the vertebral trabecular bone (see Vertebral Strengths, below). The superior and inferior margins of the vertebra, called vertebral endplates, average less than 0.5 mm in thickness (244a). In the young adult a thin layer of hyaline cartilage about 1 mm thick covers the central region of the endplate. Neither the vertebra nor the endplate is rigid. Studies have shown that under a 7500-N compressive load (as might occur in heavy lifts), the endplate can deflect up to 0.5 mm, reflecting a strain in the central vertebral trabecular bone of up to 3% (53).

Upper Cervical Vertebrae

The structures of the C-1 and C-2 vertebrae are highly specialized to facilitate a wide

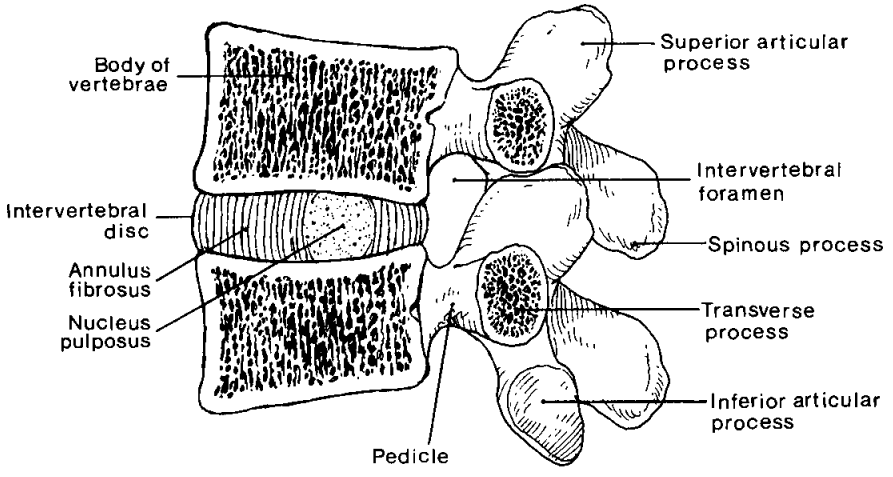

FIG. 2. Lumbar spine motion segment. Medial view of right half when sectioned in the midsagittal plane. Ligaments are omitted for clarity.

range of movements of the head (occiput). For this reason, their forms differ markedly from those of the other vertebrae. The C-1 vertebra, which supports the skull, is a ring-shaped bone with well-developed superior facet joints. The centrum of C-2, the dens, is elongated vertically and forms a longitudinal axis about which C-1 and the occiput rotate. The motion around this axis is constrained by the strong transverse and odontoid ligaments and the Occ–C1 and C1–2 facet joints. The biomechanical role of the alar ligaments has been investigated using both experimental (196) and computer simulation (115) studies. It has recently been shown, for example, that both alar ligaments must be intact to limit axial atlantoaxial joint rotation (71).

Intervertebral Disk

The largest avascular structure in the human body, the intervertebral disk, acts as a flexible spacer between adjacent vertebrae and carries significant compressive loads resulting from gravitational and muscular forces. Contrary to what was thought some years ago, the disk does not behave as a thin-walled cylinder under internal hydraulic pressure. Rather, the normal disk behaves as a thick-walled, deformable annulus, which until degenerate, contains fluid under pressure (117).

The disk consists of two regions, the inner nucleus pulposus and the outer annulus fibrosus (Fig. 3). The nucleus pulposus is formed from a strongly hydrophilic proteoglycan gel that is enmeshed in a random collagen matrix. Marchand and Ahmed showed that the annulus consists of 15 to 26 distinct layers of discontinuous concentric lamellae, the thicknesses of which increase markedly with age; they are arranged so that the orientation of the collagen fibers relative to the longitudinal axis of the spine alternates in successive layers (148). When they viewed the annulus from above, they reported many discontinuities: in any 20° circumferential sector, approximately half the laminae terminate or originate. When the annulus is viewed radially, the collagen is seen to be arranged in 20 to 60 bundles over the height of the disk. From the periphery inward, the proportion of type I collagen decreases, whereas that of type II increases (49,93). The lamellae become progressively less distinct as they merge with the central nucleus pulposus. Systematic radial and circumferential variations in its mechanical properties have been ascribed to variations in regional biochemical composition and structural properties (36,246) as well as to its poroelastic behavior (133).

In adults, the proportion of type I collagen in the posterior annulus progressively increases in the three caudal lumbar levels (48). This has been taken as possible evidence for remodeling of the disk structure in response to stress.

When an axial load is applied to a disk, the external forces are resisted by several mecha-

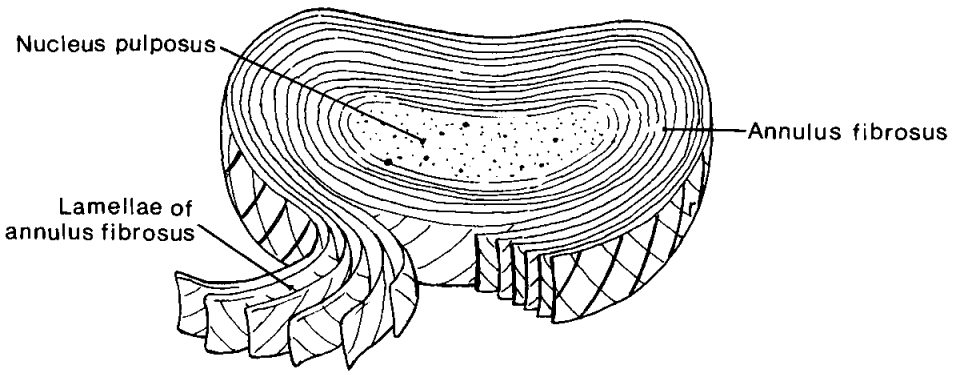

FIG. 3. Intervertebral disk sectioned to expose the annular organization.

nisms, including an elevated nucleus pressure (174). When the disk is in a steady state of hydration, the osmotic swelling pressure developed by the hydrated proteoglycans contained in the nucleus balances the applied stress. If the applied stress increases, water is driven out of the disk until a new steady state is reached. If, on the other hand, the applied stress is reduced, the disk rehydrates accordingly (Fig. 4). Disks taken at surgery have been shown to have a lower fluid content in the nucleus and higher fluid content in the outer annulus than disks removed at autopsy, presumably because of minimal applied compression loading (257). Under compression, the nucleus loses water over time. For example, Adams and Hutton (5) have shown *in vitro* that in 4 hr the annulus and nucleus can lose up to 15% and 10% of their free water, respectively. Cyclic compression loading can further increase this loss and consequently decrease disk height by a factor of two (293); it is partly responsible for the well-known diurnal changes in standing height (80).

Ecklund and Corlett (87) have shown *in vivo* that the total decrease in disk height that occurs after standing for 1½ hr can be regained in about 15 min by lying supine. These workers found that over the course of a day the total spinal height loss can reach about 1 cm, especially if heavy loads are lifted. The loss in height can be described by a Kelvin spring–dashpot model and is given by $y = A_1 + A_2e^{-kt}$, where t is time and A_1, A_2, and k are de-

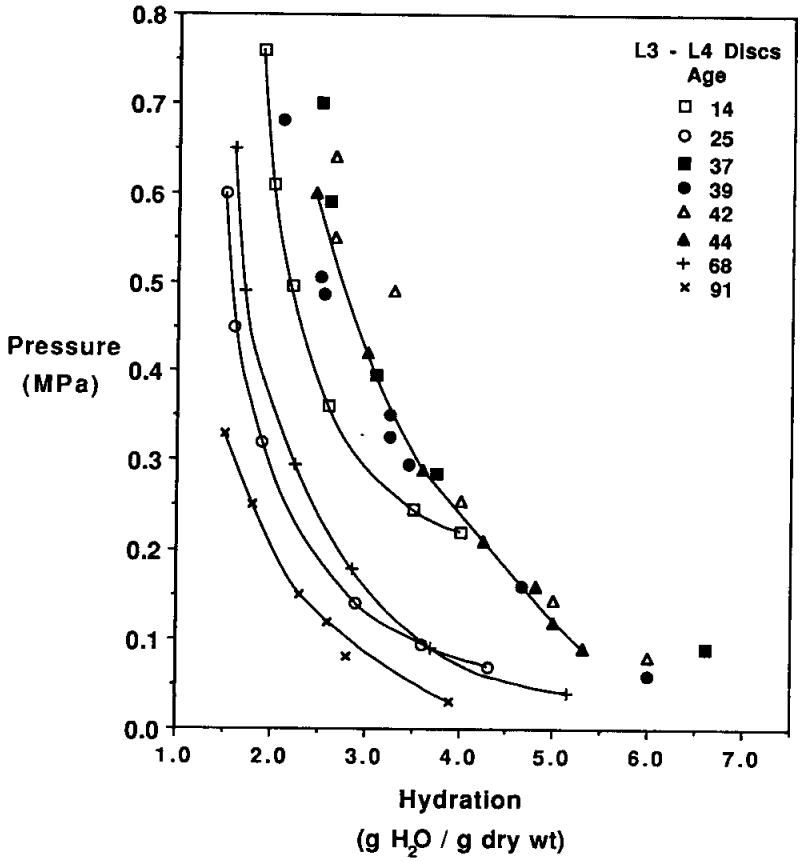

FIG. 4. Human intervertebral disk hydration versus osmotic swelling pressure. (From Urban and McMullin, ref. 277, with permission.)

termined experimentally. For example, in one subject, A_1, A_2, and k were found to be 1876.5 mm, 14.1 mm, and 0.186 hr^{-1}, respectively.

The maximum cell density in the disk is known to be determined by the nutritional supply (240). Nutrition of the disk is accomplished by diffusion through two main routes: via the blood vessels surrounding the annulus and via the capillary beds adjacent to the cartilaginous endplates. The area of the endplate available for diffusion is approximately 40% of the total vertebral area (72,113,276). Matrix synthesis of ^{3}H-proline and ^{35}S-sulfate in the bovine coccygeal disk has been found to be highest at the inner annulus and lowest in the outer annulus (192); those rates were load sensitive, increasing with increasing load and then decreasing on further load. Further work is needed to understand how changes in disk nutrition associate with degenerative changes commonly found in the annulus and endplates. Sclerotic bone associated with endplate fractures might well be expected to adversely affect the efficacy of the endplate diffusion route, for example.

Facet Joints

The main role of the facet joints is to limit excessive intervertebral shear and torsion motions of the intervertebral segment. Although much low-back pain in the young adult may be discogenic in origin, in the older spine with degenerative changes it is possible that the facet joints, relatively small posterior structures, may also be involved. Investigators have noted the rich afferent innervation of the facet capsules with the associated possibilities for signaling pain (25). Moreover, conditions such as spondylolysis seem to stem from a fatigue fracture of the posterior elements.

There is a gradual and characteristic change in the three-dimensional orientation of the facet joint surfaces from the cervical region through the thoracic region to the lumbar region (199,292). The kinematic constraints provided by the facet joints are particularly pronounced in the cervical spine, where they cause marked coupling between lateral bending and axial torsion motions. This is the only region where such coupling is significant. The facet joint surfaces themselves are often nonplanar. In the upper lumbar spine, the opposing surfaces of the facet joints are oriented approximately in the sagittal plane, thus limiting axial rotation. More caudally, their orientation is almost in the frontal plane. Computerized tomography (CT) scans can be used to measure the angles subtended by the facet joint surfaces. For example, the average angle between left and right facet surfaces in the transverse plane increases from 74° at L3–4 to 96° at L4–5 and 106° at L5–S1 (278). However, large variability exists at the L5–S1 level: values ranging from about 36° to 180° have been reported (26). In the lumbar spine the area of each facet ranges from 100 to 350 mm^2 and varies with facet orientation (94). The right and left facet joint orientations are not necessarily symmetric about the midline. For example, in 3000 spinal radiographs, 23% of patients exhibited asymmetry at the three lower levels (46). Most patients showed asymmetry of less than 10°, but facet asymmetry, known as facet tropism, can range up to 42° (94). *In vitro* studies show that simultaneous compression and anterior shear cyclic loading can lead a vertebra to rotate to the side of the more oblique facet (75).

The mechanical properties of the lumbar facet joints were studied by Skipor and coworkers (247) in order to estimate the loads carried by the facet joints in different situations. One way of estimating the amount of load sharing between the disk and the facets is by using mathematical models (15,241,242, 297). These models are usually validated by comparing predicted behavior (with and without posterior elements) with experimental measurements (see Motion Segment Stiffnesses, below). These studies show that the facets carry 10% to 20% of the spinal compressive load in an upright standing position and more than 50% of the anterior shear load on the spine in a forward-flexed position. The facets have been shown to resist anterior shear forces up to 2 kN without failure (76).

The contact pressure between facet joint surfaces can be measured *in vitro* by introducing a pressure-sensitive film that registers the average pressure over time or by using a miniature pressure transducer to record the instantaneous fluid pressure under load in this fluid-containing synovial joint (90,142). These techniques have been used to demonstrate that in torsion the facet under compression was loaded most heavily. The relationship between the applied moment and experimentally measured pressure increased linearly and ranged from 4 to 26 Nm/kPa among specimens. The highest facet pressures were recorded under combined torsion, flexion, and compression. Facet joint pressures also increased with a reduction in disk height; the average peak pressure was found to rise 36% for a 1-mm loss in disk height, and 61% for a 4-mm loss in disk height (85).

By categorizing the loads carried by the facets in carefully controlled experimental conditions, studies such as these may help to suggest or clarify the etiology of clinical disorders, and may answer questions such as whether spondylolysis is caused by fatigue fracture of the pars interarticularis (74).

Sacroiliac Joints

Reviews of the literature describing the anatomy and morphology of the sacroiliac joints and their articular surfaces and associated ligaments are given by Ashton-Miller and colleagues (22) and Vleeming and colleagues (282,283).

Vertebral Strengths

Many measurements of vertebral compression strength have been made (291). These studies show an increase in compression strength as one moves caudally, from 1.5 kN at C-3 to 2.0 kN at T-1, 2.5 kN at T-8, 3.7 kN at T-12, and to 5.7 kN at L-5. The ultimate vertebral compressive strength has been shown to increase by 380 N from L-1 to L-4 (109). McBroom and colleagues (152) demonstrated that most of the vertebral ultimate compressive strength is derived from the strength of the cancellous bone; removing the entire cortex weakened the vertebra by only 10%. Variation in ultimate compressive strength between individuals can be large in adults. For example, Hutton and co-workers (118) found a range greater than one order of magnitude, from 0.8 kN to 15.6 kN. Recently, Brinckmann and co-workers (51) showed a linear correlation between ultimate compressive strength of lumbar vertebrae and a parameter equal to bone density times endplate area, as determined by CT scanning. The ultimate compressive strength has been estimated to within 1-kN accuracy using CT methods (52). Because bone density was found to remain essentially constant throughout the thoracic and lumbar spine, the craniocaudal increase in ultimate compressive strength results from the increase in cross-sectional area of the vertebrae. Brinckmann and colleagues have demonstrated convincingly that the fatigue life of vertebrae, indicated by the initial endplate failure, depends on the compressive load range (Table 1). This has implications for setting guidelines for safe repetitive lifting in the work place. Quantitative computed tomography is a useful technique for estimating the fatigue strength of vertebrae *in vivo* because of the ease with which bone density and endplate area can be estimated. The probability of failure *in vitro* within 5000 cycles, estimated to be equivalent to 2 weeks of athletic training, increases from 36% at a loading range 30% to 40% of ultimate compressive strength (UCS) to 92% at a loading range of 60% to 70%

TABLE 1. *Probability (%) of vertebral fatigue in the lumbar spine*

Load level (%UCS)[a]	Cycles of failure				
	10	100	500	1000	5000
30–40%	0	0	21	21	36
40–50%	0	38	56	56	67
50–60%	0	45	64	82	91
60–70%	8	62	76	84	92

[a]UCS, ultimate compressive strength. Data from Brinckmann et al. (51).

UCS. Vertebral bone mineral density has also been shown to correlate with trunk extensor muscle strength (244). Hence, it is reasonable that competitive weight lifters exhibit significantly increased vertebral bone mineral density (103) due to adaptive remodeling of their vertebrae caused by exposure to large loads.

Motion Segment Stiffnesses

Knowledge of the load-displacement behavior of the spine and its components is required for biomechanical analyses of spine function. For convenience, tests of spine mechanical properties have traditionally used short lengths of spine consisting of two vertebrae and their intervening soft tissues. These are called spine motion segments or spine functional units. In most cases the load-displacement properties are obtained by gripping the lower vertebra securely, applying known test forces or moments or both to a point on the upper vertebra, and measuring the resulting displacements (195). In this way the coefficients of the flexibility matrix can be measured directly. Table 2 gives averaged stiffness values for each spine region. Load-displacement data have also been recorded for whole spine segments, including the complete ligamentous lumbar spine. In the next four sections we consider the load-displacement behavior of each region of the spine.

Cervical Spine

The properties of the occiput–C1–C2 complex were studied for the first time by Goel and co-workers (100). They found that a test moment of 0.3 Nm produced rotations ranging from only 3° in lateral bending to 14.5° at Cl–2 in axial torsion and 16° at Occ–C1 in extension. Translations occurring in these upper segments under loads up to 1.5 Nm have also been reported. Moroney and colleagues (167,168) found lower cervical spine motion segments to be an order of magnitude stiffer than upper cervical segments. Stiffness was greatest in axial torsion and least in flexion.

Many severe neck injuries are associated with vertebral body fractures as well as intervertebral joint dislocations resulting from a sudden flexion–compression loading of the cervical spine (262,298). The presence of a compression fracture is evidence that the axial compressive load exceeded the ultimate compressive strength of the vertebrae. *In vitro* tests of complete intact cervical spine specimens have shown that commonly observed cervical fractures can be produced under conditions in which the cervical spine lordosis is removed and the spine is rapidly loaded under axial compression (300). Under such conditions the cervical spine can fail by buckling (208): with the head constrained at impact, an anterior, posterior, or lateral "bowing" of the middle cervical region can occur under the compression loading. The direction in which it buckles will be determined principally by how the head is constrained (173) at impact as well as the axis of least cervical bending stiffness (for example, flexion, extension, or one of the two lateral bending directions). Although there is no time for the cervical muscles to respond during most impact loadings of the cervical spine, anticipatory pretensing

TABLE 2. *Average stiffness values (N/mm and Nm/deg) for the adult human spine*

Spine level	Comp	Shear (ant/post)	Lat	Bending (flex/ext)	Lat	Axial torsion	Reference
Occ–C1	—	—	—	0.04/0.02	0.09	0.06	100
C1–2	—	—	—	0.06/0.05	0.09	0.07	100
C2–7	1317	125/55	33	0.4/0.7	0.7	1.2	168
T1–12	1250	86/87	101	2.7/3.3	3.0	2.6	195
L1–5	667	145/143	132	1.4/2.9	1.6	6.9	34, 237
L5–S1	1000	78/72	97	2.1/3.0	3.6	4.6	159

of muscles up to about 50% of their maximum activation can result in a fivefold increase in muscle stiffness (125,245), thereby increasing instantaneous spine-bending resistance. Although this muscle stiffness will increase spine resistance to buckling, it comes at the cost of also increasing spine compression (see section on Biomechanical Model Analyses for mechanism by which spine muscle activity increases spine compression). Experimental and theoretical studies are therefore needed to investigate how the threshold for spine fracture is affected by the level of cervical spine muscle coactivation immediately before and during impact.

Thoracic Spine

The properties of the isolated adult thoracic spine have been reported by Panjabi and colleagues (195) and others. They found average stiffness values ranging from 100 N/mm in lateral shear to 900 N/mm in anterior or posterior shear to 1250 N/mm in compression. Rotational stiffnesses were about 2 to 3 Nm/° in flexion, extension, lateral bending, and axial torsion.

Lumbar Spine

The overall static load-displacement behavior of lumbar spine motion segments has been well documented (34,237). In these studies, the stiffness of intact spine motion segments was in the range of 600 to 700 N/mm in axial compression and 100 to 200 N/mm in anterior, posterior, or lateral shear; however, there was considerable intraindividual variation. Test forces ranged from 86 N in shear to 400 N in compression and were applied at the vertebral body center. Rotational stiffnesses ranged from 1.0 to 2.0 Nm/° in flexion, extension, and lateral bending and 6.8 Nm/° in axial torsion when test moments of 4.7 Nm were used. To simulate the compression loading of the spine *in vivo,* these results were obtained with a 400-N compressive preload. More recently, the lumbosacral (L5–Sl) spine motion segment has been found to have lower shear stiffnesses (0.5 to 0.75 times), larger bending stiffnesses (1.4 to 3.3 times), and less stiff torsion resistances (1.5 times) than L1–5 lumbar segments (159). We have demonstrated that compressive preloads of the magnitude likely to act *in vivo* can lead to a significant stiffening of the motion segment (123).

The influence of the posterior elements has been investigated by first testing intact motion segments and then excising the pedicles and retesting the motion segment without the posterior elements. Not surprisingly, this always leads to a decrease in stiffness. For example, McGlashen and co-workers (159) found that removal of the posterior elements resulted in 1.7-fold increase in shear translations in response to a given shear force, a 2.1-fold increase in bending rotations in response to a given moment, and a 2.7-fold increase in axial rotation in response to a given axial torsion moment. The behavior of lumbar motion segments under larger shear and with bending and torsion loads of up to 1000 N and 100 Nm have also been examined. Although shear load-displacement behavior remained linear, moment behavior was found to be slightly nonlinear at the higher loads (23).

The mechanical response of the disk to loads has been measured in terms of both internal and external strains. Stokes and Greenapple (258) used a photogrammetric technique to measure surface strains of the annulus fibrosus. Some of the larger strains were measured under torsion, where a 17-Nm load resulted in tensile strains of 9%, well under the 25% ultimate strain of the annulus in tension. Martin and colleagues (149) used an array of 0.5-mm-diameter steel spheres to visualize the movements of the annulus and nucleus under various loads. With a resolution of 0.125 mm, the method showed that the nucleus moves posteriorly in flexion and anteriorly in extension. Disk bulge under load, of course, has clinical relevance for sciatic and stenotic symptoms. *In vitro* (216), the typical increase in disk bulge under load is small: less than 1 mm of bulge under 1000 N compres-

sion. Posterior disk bulge is greatest in extension and least in flexion.

Sacroiliac Joints

The mechanical properties of the sacroiliac joints (35,106,249) have received little attention compared to their anatomic, histologic, and clinical characteristics, which were reviewed extensively by Bellamy and co-workers (31). Adult sacroiliac joints were found to exhibit stiffnesses of 100 to 300 N/mm for superior, inferior, anterior, and posterior shear of the sacrum relative to the ilium. Bending stiffness was lowest in axial torsion, 7 Nm/°; higher in extension, 12 Nm/°; and largest in flexion and lateral bending, 16 and 30 Nm/°, respectively (22). Thus, depending on the test direction, these joints have from 0.05 to 7.00 times the stiffness of intact L1–5 lumbar motion segments. No test data are available for the load-displacement behavior of the pubic symphysis. The effects of joint stiffness and pelvic dimensions on mechanical behavior of the intact pelvis have been investigated by Scholten and co-workers using models (221). The recorded motions of these joints *in vivo* is modest: namely, one or two degrees (259). A novel hypothesis, which still requires experimental testing, has been been advanced concerning the stabilization of the sacroiliac joints in physically strenuous upright activities through the coordinated activity of the trunk, pelvic, and hip muscles; these structures are thought to exert a medially directed resultant load on the joints, forcing their articular surface irregularities to "interlock," thus increasing their resistance to the significant cephalocaudad shear loads (282).

Rib Cage Components

The load-displacement properties of adult ribs and costovertebral and costosternal articulations have been measured. In general, for the costosternal articulations, a 7-N test force applied at a point 1 cm lateral to the cartilage gave rise to displacements of about 5 to 20 mm in the superior/inferior or anterior/posterior directions (233). Similarly, for the costovertebral articulations, the same test load applied to the rib about 5 cm from the vertebral body resulted in similar displacements of the loading point in the anterior/posterior and superior/inferior directions but only 1-mm displacement in the lateral direction. Human ribs are themselves flexible. A 7-N test force applied transversely to the end of a rib whose other end is gripped securely causes displacements of about 30 and 60 mm in upper and lower thoracic ribs, respectively (232). These data have been used to validate computer models of the ribcage under various types of loads (see section on Biomechanical Model Analyses).

Ligaments

Spinal ligaments pass between each vertebra along the length of the spine and function to limit excessive joint motion. These ligaments include the anterior and posterior longitudinal ligaments, the ligamentum flavum, the inter- and supraspinous ligaments, and the intertransverse ligaments. The facet joint capsules also act as tension-bearing structures between the articular processes (247). Although most ligaments run the length of the spine, the supraspinous ligament does not extend caudally past L-5 (112).

The tensile properties of isolated spinal ligamentum flavum have been reported by Nachemson and Evans (176); Tkaczuk (269) studied the anterior and posterior longitudinal ligaments, and Waters and Morris (288) have studied the inter- and supraspinous ligaments. Ligamentum flavum demonstrated a pretension in the range of 5 to 18 N, depending on age, and a failure stress in the range of 2 to 10 MPa at strains of 30% to 70%. The longitudinal ligaments failed at about 20 MPa, carrying loads of 180 N (posterior) and 340 N (anterior).

One way to examine the mechanical role of ligaments in spine motion segments is to repeatedly apply a standard load, say a flexion moment, to the motion segment while se-

quentially sectioning ligaments from posterior to anterior (201). Panjabi and colleagues (197) showed that when lumbar motion segments are loaded in flexion under a moment of 15 Nm, strains in ligaments furthest from the axis of rotation can reach nearly 20%.

Hormonal factors are known to affect collagenous tissue laxity. For example, a relationship has been identified between ligamentous laxity and those women who, later in pregnancy, developed back pain (193).

Muscles

The trunk musculature, though complex, may be divided into the posterior wall musculature (erector spinae or paravertebral muscles), the respiratory or intercostal muscles between adjacent ribs, and abdominal wall muscles comprised (from inside out) of the intertransversus, the interior and exterior obliques, and, anteriorly, the rectus abdominis. The most superficial layer of trunk muscles on the posterior and lateral walls are primarily broad muscles connecting to the shoulder blades, upper extremities, and head: the rhomboids, latissimus dorsi, pectoralis, and trapezius. Finally, some of the lower trunk muscles, such as transversus abdominis, attach to a strong superficial fascial sheet, the lumbodorsal fascia, which may be thought of as a three-layered tensile load-bearing structure that inserts onto the upper pelvic borders. The anatomy of this fascia has been reviewed by Bogduk and Macintosh (42). The diaphragm is a large dome-shaped muscle attached to the lower ribs and to the thoracolumbar spine via the crura and forms the boundary between the lungs and the contents of the abdominal cavity. Its action on the spine has not been included in any model to date. The iliopsoas muscles originate on the anterior aspect of the lumbar spine to pass across the hip joint to the inside of the femur.

The histochemical composition of a muscle can determine its rate of tension development, fatigue characteristics, and power output. Vertebral muscle composition has been reviewed by Bagnall and co-workers (27), who found 50% to 60% type I muscle fibers. Interestingly, 11% more type I fibers were found on the left side of L-5 than on the right in asymptomatic persons. One possible explanation for this may be the dominance of right-handedness, which inevitably increases left-side paravertebral muscle loading.

Striated muscle is almost never injured in isometric or shortening contractions; it can be injured when it is activated and forcibly lengthened (57). Under such conditions, striated muscle can develop at least 50% larger forces than under isometric conditions (154,287), a fact that has not escaped the notice of athletes or anyone using that phenomenon to jerk a heavy load off the ground, hence increasing the potential for injury to the ultrastructure of specific sarcomeres. Depending on the severity of the injury, 1 to 4 weeks is required for the complete recovery of the muscle structure and function (56). That this time span is consistent with the clinical finding that 33% of patients with acute back pain reported pain lasting less than 1 month (81) should not be overlooked. It is therefore instructive to consider situations in which back muscles might be forcibly lengthened and therefore placed at risk for injury.

Problem

Give an example of the conditions under which one might expect the erector spinae to be at greatest risk for injury. For simplicity, consider a sagittally symmetric task.

The erector spinae are most likely to be injured when they are used in a strenuous effort to decelerate the trunk when it is flexing and to accelerate it into extension. Consider what happens, for example, following a trip that leads to a severe stumble or fall. Once the trip is detected the erector spinae become maximally active in an attempt to arrest the forward momentum of the trunk. Let us assume that the level of neural recruitment is maximal. The erector spinae are undergoing a lengthening contraction, and the tension they develop will rise above maximal isometric values in proportion to their initial rate of elongation (65).

Finally, when that force has acted long enough to arrest further trunk flexion, it will lead to trunk extension relative to the pelvis. The greatest risk for muscular injury occurs at the instant of peak erector spinae tension (57), because that is when the internal stress is greatest. The later section on Biomechanical Model Analysis will use mathematical models to explain why this peak tension in turn places the vertebrae under considerable compression loading, so much so that the vertebrae in some individuals can be placed at risk for a fracture.

Mathematical models of the spine often require detailed descriptions of the origin and insertion points of muscles and muscle slips, their anatomic and physiological cross-sectional areas, and even their fiber lengths and fiber types. For example, none of the lumbar back muscles can exert torsional moments greater than 2 Nm about the lumbar spine: it is the oblique abdominal muscles that are the principal axial rotators of the trunk (145). The detailed anatomy of trunk muscles is being updated continually (41,43,44,134,166). Intraindividual differences and changes in muscle lever arms with different body postures may now be taken into account (144,190,273, 275). Magnetic resonance imaging has led to the *in vivo* estimation of muscular lever arms about the cervical and lumbar spine (157,184, 270,273), although the lines of action of muscle fibers in muscles such as the erector spinae remain difficult to visualize because spatial resolution remains limited in whole body images.

Nervous System Tissues

Relatively little attention has been given to the biomechanics of neural tissues associated with the spine. Olmarker and collaborators (192) have studied the effect of pressure on intrathecal spinal nerve root blood flow. Certain movements of spine motion segments are known to affect the foraminal area available for the exiting spinal nerve roots. For example, extension reduces the size of the foramen by at least 20% (202). In some older individuals with spinal stenosis, this can cause nerve root entrapment (220), resulting in sciatic symptoms on standing and in trunk extension (252). This phenomenon is primarily a compression phenomenon and contrasts with a second mechanism that can cause sciatic symptoms in younger and middle-aged adults in relation to tension in the nerve root. To understand this we examined the mechanical factors that determine *in situ* the contact force between a spinal nerve root and a simulated disk protrusion (254,256). Those studies describe the trilamellar arrangement of Hoffmann ligaments that constrain the thecal sac and nerve root above the disk, while the foraminal attachments are known to constrain the extrathecal nerve root distal to the disk. Because the nerve root is thereby constrained above and below the herniated disk, much like a stiff rubber band stretched over the protrusion, the contact force tending to compress the nerve root unilaterally was found to increase with increasing simulated disk protrusion magnitude, even for increases in protrusion of as little as 1 mm. It was also found to increase with increasing disk height and to decrease with decreasing disk height. Because of the known diurnal loss in disk height over the course of the day (see Intervertebral Disk) (212), the latter explains the clinical finding that patients whose sciatica is related to nerve root tension commonly report sciatic symptoms as being worst in the early morning and less severe after an hour of being upright. It also helps to explain why, when chemonucleolysis is effective in alleviating sciatic symptoms, success is almost always correlated with a disk height reduction induced by the chemonucleolysis (253).

MEASUREMENTS OF SYSTEM BEHAVIOR

Spine Configuration

The spine is approximately straight when viewed frontally because each vertebra and disk is approximately symmetric about the

sagittal plane. A slight lateral deviation or scoliosis is common because no structure in the body has perfect symmetry. In a lateral view, the spine exhibits four curves (127). In the cervical and lumbar spine, each curve is concave backward-a lordosis. Cervical lordosis ranges from 2° to 24° with an average of 9° (102). In the thoracic and sacral spine, each curve is concave forward kyphosis. The thoracic kyphosis normally averages 39°, with 93% of kyphoses ranging from 22° to 56°. Most of the thoracic kyphosis results from slight wedging of the vertebral bodies; a thoracic disk tends to have endplates that are approximately parallel (284). Wedging over three or more thoracic vertebrae that exceeds 15° is considered abnormal and occurs in conditions such as Scheuermann's kyphosis. Normal lumbar lordosis averages 57°, with 93% ranging from 38° to 75° (284). There are no significant differences in the angle of lordosis between males and females (95).

The lumbosacral angle was defined by Ferguson as the angle that the plane of the upper S-1 endplate makes with the horizontal. In an upright stance, this angle averages 41° in the adult male, with 95% of individuals lying within the range of 26° to 57° (110).

Anthropometry

Anthropometry is the study of human size and form. Mathematical models of the spine often require the linear dimensions and shape of the spine and trunk as input data. These may be obtained from a variety of sources.

Lanier (135) examined the overall geometry of macerated vertebra; Brandner (47) studied disk and vertebral dimensions during growth. On a more global scale, marked variations exist between individuals: Fig. 5 demonstrates the variation in sagittal curvatures of a sample of 18 adolescent girls with a mean age of 12 years. The equation of a fifth-order

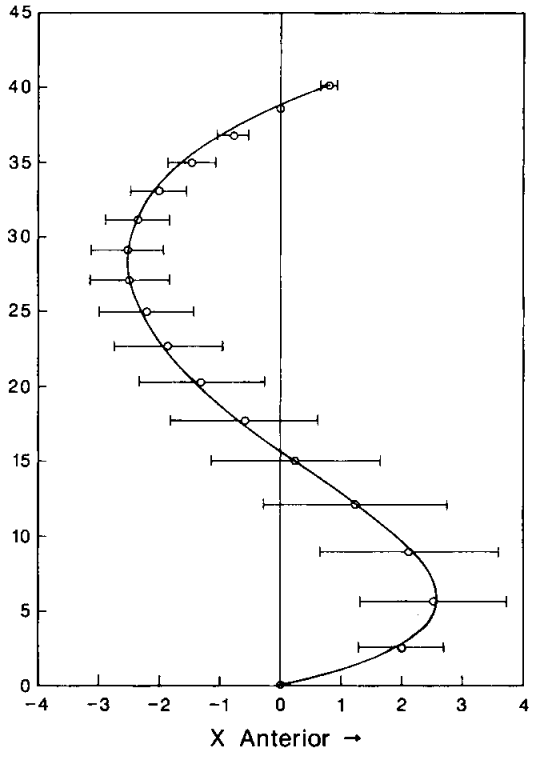

FIG. 5. Normal variation in shape of the adolescent spine. Mean (denoted by *o*) and standard deviation (denoted by *bars*) of vertebral center coordinates (cm) are given. Note that the *y* axis is oriented vertically and the *x* scale is expanded. *Solid line* is fifth-order regression line whose equation is given in section entitled Anthropometry. Data are for 18 adolescents between the ages of 10 and 18 years of age (24).

polynomial regression ($r^2 = 0.80$) fitted to the coordinate values is

$$x = 1.02030y - 0.12767y^2 + 0.00543y^3 - 0.10504 \times 10^{-3}y^4 + 0.83552 \times 10^{-6}y^5$$

where x is the anterior offset in millimeters and y is the distance in millimeters superior from the center of S-1. Table 3 gives the average vertebral center coordinates and angle of disk inclination for these spines.

Linear and cross-sectional dimensions can be measured directly from subjects using calipers (161). These have been used to scale cadaveric segmental mass and inertia data from other sources, such as Clauser and colleagues (64) or McConville and co-workers (153).

Ranges of Motion

Many techniques have been developed to measure spine range of motion *in vivo*. Most are noninvasive and use measurements from surface landmarks (165), pantographs (294), and goniometry (89). Although often quick and convenient, these techniques yield results that are reproducible only to within 7% to 12% (163). They give a reasonable approximation of total spine motions but a poor indication of actual intersegmental spine motions and so are not as reliable for the latter purpose as radiologic techniques (150,211). For this reason we review only radiologic data (Table 4).

Lumbar Spine

Perhaps the most thorough range of motion studies of the lumbar spine region are those of Pearcy and Tibrewal (206) and Pearcy and collaborators (204). These workers carefully standardized test subject postures and used radiographic methods to determine the average maximal intersegmental rotations at L5–S1. In flexion and extension these were found to be 9° and 5°, respectively, whereas in axial rotation and lateral bending, the average was 2° and 3°, respectively.

Thoracic Spine

One of the only studies of thoracic range of motion is that of Bakke (28), who found that total intersegmental flexion–extension movement does not exceed 5°. At each end of the thoracic spine, the motions are similar to those of the cervical and lumbar regions (28). In lateral bending, motions are limited to 4° or less.

TABLE 3. *Mean (SD) coordinates of vertebral body centers in healthy individuals*

Level	x (cm)	y (cm)	θ (°)[a]
T1	0.80 (0.22)	40.13 (0.15)	26.85 (7.75)
T2	0.0	38.47	26.85 (6.12)
T3	−0.77 (0.17)	36.78 (0.11)	24.03 (5.13)
T4	−1.46 (0.33)	35.01 (0.19)	20.03 (4.97)
T5	−2.01 (0.44)	33.11 (0.34)	15.35 (4.33)
T6	−2.36 (0.49)	31.17 (0.33)	9.39 (3.41)
T7	−2.52 (0.59)	29.15 (0.39)	3.82 (3.98)
T8	−2.49 (0.64)	27.07 (0.41)	−2.40 (4.03)
T9	−2.32 (0.75)	24.90 (0.38)	−6.57 (4.54)
T10	1.86 (0.89)	22.64 (0.40)	−8.95 (5.19)
T11	1.31 (1.02)	20.25 (0.37)	−11.22 (5.49)
T12	−0.60 (1.22)	17.72 (0.31)	−12.33 (5.76)
L1	0.24 (1.40)	14.99 (0.35)	−13.40 (4.94)
L2	1.22 (1.50)	12.10 (0.40)	−13.43 (4.65)
L3	2.11 (1.45)	8.96 (0.44)	−8.18 (4.42)
L4	2.51 (1.18)	5.46 (0.47)	2.07 (7.57)
L5	1.99 (0.69)	2.48 (0.40)	19.13 (11.00)
S1	0.0	0.0	42.46 (10.57)

[a]θ is the inclination of the upper endplate with the x axis, which is horizontal; a positive angle denotes an inclination below the horizontal. Data from Ashton-Miller and Skogland (24).

TABLE 4. *Average segmental range of motion (°) at each spine level*[a]

Level	Flexion	Flexion/ Extension	Extension	Lateral bending	Torsion
Occ–C1	13[b]		13[b]	8[b]	0
C1–2	10[b]		9	0[b]	47
C2–3	8		3	10[b]	9
C3–4	7		9	11	11
C4–5	10		8	13	12
C5–6	10		11	15	10
C6–7	13		5	12	9
C7–T1	6		4	14	8
T1–2	5		3	2	9
T2–3		4		3	8
T3–4		5		4	8
T4–5		4		2	8
T5–6		5		2	8
T6–7		5		3	8
T7–8		5		2	8
T8–9		4		2	7
T9–10		3		2	4
T10–11		4		3	2
T11–12		4		3	2
T12–L1		5		3	2
L1–2	8		5	6	1
L2–3	10		3	6	1
L3–4	12		1	6	2
L4–5	13		2	3	2
L5–S1	9		5	1	1

[a]Cervical and thoracic data from ref. 291. Cervical data from ref. 132 unless otherwise specified. Thoracic data from ref. 28. Values are total flexion/extension values. Lumbar data from refs. 204, 206.

[b]Data from ref. 291, p.65.

Torsional data are not available, probably because of difficulties of measuring planar radiographs to a precision of better than 5° (84).

Cervical Spine

Kottke and Mundale (132) studied the range of motion of the lower cervical vertebrae *in vivo* (Table 4). Ranges of motion for the upper cervical spine have not been thoroughly documented (86), but estimates are given by White and Panjabi (291).

Measurements of Intact Trunk Properties *In Vivo*

The bending stiffness of the trunk has been measured *in vivo* in flexion by Scholten and Veldhuizen (222). They applied three-point bending forces to the trunk, which was supported at the pelvis and shoulder region. Bending stiffness was found to be 0.153×10^8 N/mm^2 or roughly ten times that of the isolated spine. This illustrates how much the rib cage, fascia, and passive muscle tissues serve to stiffen the isolated spine, even in the fully relaxed supine individual.

Trunk Proprioception

Upright posture in humans requires the head to be maintained over the pelvis. The neuromuscular motor control system responsible for this relies on afferent feedback from many sources, including the spine and trunk articular, muscular, and cutaneous sensors as well as the vestibular organs. Trunk proprioception, the ability to sense where the top of the spine is relative to the pelvis, is thus derived from this feedback. Some patients, such as children with certain types of scoliosis, can unknowingly develop a lateral trunk "imbal-

ance" whereby T-1 is offset laterally from S-1 by several centimeters. Why such patients can not sense their asymmetric posture is presently unknown. Indeed, relatively little is known about the accuracy of trunk proprioception, even in the healthy individual. Ashton-Miller and colleagues (17) showed that trunk proprioception improves with age in healthy children so that by adulthood, the top of the spine can be reliably repositioned within 1° of the upright. For a flexible column with some 25 joints, this is impressive accuracy. The threshold for detecting axial torsion is less than 1° (263), whereas proprioceptive accuracy has been found to be slightly worse in the sagittal plane than the frontal plane (158). To examine mechanisms, trunk proprioception acuity has also been compared with the spine in the vertical plane and in the horizontal, gravity-free, plane (122).

Disk Injury

One of the most common causes of back and extremity pain is compression of the dura and/or nerve roots by disk prolapse, particularly in the cervical region and at the lowest lumbar levels. It is not known what causes a disk to prolapse. Disk protrusion and subsequent prolapse may be related to excessive loading that leads to disk degeneration and fatigue failure of the inner posterior annular fibers (4,7,49). Two studies have identified a genetic predisposition to disk herniation in the young (213,279), and a recent study in adults has demonstrated that the odds ratio of a lumbar disk herniation is approximately tenfold higher in relatives of a patient with a proven disk herniation than in matched controls (217). The mechanism of genetic expression is presently unknown. For example, except for a possible association between lifting free weights and cervical prolapse, sports such as recreational baseball, softball, golf, bowling, swimming, diving, jogging, or racquet sports do not seem to be associated with an increased risk for disk herniation (172). Even disk degeneration, as scored by magnetic resonance (MR) imaging, was not significantly more extensive in men who exercised more than two times per week for 24 years than in their identical twin who exercised significantly less (280).

A recent review (2) of the quasistatic loading conditions known to cause posterior disk prolapse examined combined axial compression, flexion, and lateral bending. Such loading can cause up to 50% increases in the tensile strain in the posterior annulus (205), significant posterior annulus thinning (6), and increased hydrostatic pressure in cadaver lumbar disks. Cyclic loading of the disk in combined flexion, rotation, and compression at 1.5 Hz has been shown to produce annular protrusion and/or prolapse *in vitro* in an average of only 7 hr (274). Abrupt increases in axial compression combined with hyperflexion have also been shown to cause vertebral failures (160) and failure of the posterior annulus in previously intact lumbar disks (3,4). This is supported by computer simulations that have identified annulus fibers as being particularly susceptible to failure under large lumbar anterolateral bending loads (239). A recent study suggests that disk prolapse may occur relatively late in the degeneration process, after radial fissures have formed in the annulus. These fissures are thought to form conduits along which disk fragments may be expelled with motions involving less than 10° of rotation (55). It is worth noting that these findings generally pertain to lumbar disks from cadavers under 50 years of age; the absence of hydrostatic nuclear pressure in the more degenerate lumbar disks of older cadavers usually precludes this type of discal injury because of the fibrocartilaginous nature of their nucleus. A different mode of failure can, however, occur in older disks involving inward (238), not radial, buckling of the inner annulus under compressive loading (107,261), as a result of the absence of nuclear hydrostatic pressure. In one possible scenario, this could result in a fatigue failure of the inner annulus fibers on repeated loading with damage accumulation because of little or no remodeling potential in that region.

Several studies have attempted to investigate how changes in disk integrity can affect the

load-displacement behavior of the disk and spine motion segment (198). Brinckmann and colleagues (51) found that sectioning the posterior inner annulus fibers to within 1 mm of the periphery results in a small localized bulge of only 0.5 mm in that region under compression loading, a clinically irrelevant amount. This evidence supports the argument that the adult annulus acts as a thick-walled rather than a thin-walled cylinder. On overload, they found, the endplate failed before the injured annulus failed. These findings are consistent with endplate failure as a possible precursor to disk degeneration because such a failure may disrupt disk nutritional pathways from the vertebra. However, the links among endplate failure, symptoms, and pain are not well established. Experimental models of disk degeneration have been produced by incising the outer annulus of quadruped disks (8,136,141,162,194, 207): although the site of the original outer annular injury heals with fibrocartilage, the disk degenerates within a few months with lasting structural and compositional changes.

In quadruped animals, the enzymatic removal of the nucleus pulposus by injection has been found to cause a significant loss in disk height and an increase in disk flexibility in bending and torsion (255,285). Moreover, changes in facet joint cartilage have been demonstrated subsequent to enucleation (45). This is one model of disk degeneration that seems useful clinically because disk degeneration usually precedes derangement of the facet joints (58).

Finally, another type of disk injury that can occur is related to failure of the superior or inferior endplate, usually from failure of the underlying cancellous bone. Because the elasticity of the cancellous bone returns the endplate to its original configuration when the injurious load is removed, these failures can be next to impossible to spot visually even in the sectioned specimen, let alone radiographically. Following such an endplate fracture, intraosseous pressure has been shown to increase in the vertebral body (299), a condition that has been shown experimentally to create severe low-back pain (251).

Effects of Age

Growth increases both trunk mass and inertia. Although most data on body segment mass and inertia are for adults, some estimates are available for children (124). With the advent of MR scanners, more data should become available in the future.

Not surprisingly, the immature spine is more flexible than the adult spine; the adolescent spine, for example, is from one to ten times more flexible, depending on the direction of the applied load (24). Growth also affects the angulation of the cervical facets; in the C-2 region the initial angulation of the facets to the sagittal plane increases from about 30° to nearly 80°, whereas in the lower cervical spine the change is from about 60° to 80° (191).

Growth has only a subtle effect on the magnitude of thoracic kyphosis or lumbar lordosis. Thoracic kyphosis decreases by 11% and 13% in boys and girls, respectively, between 8 and 11 years and increases thereafter by 28% and 27%, respectively, by the age of 16 years (295). Lumbar lordosis increases by about 10% from the age of 7 to 17 (284). During this time the spine increases in length by about 26% (248).

In the mature individual, cervical lordosis increases significantly in men between ages 20 and 40 (16° to 22°) and in women between ages 20 and 50 (15° to 27°) (102). In the elderly, increased thoracic kyphosis and decreased lumbar lordosis occur, partially through a decrease in overall disk height (164). This loss in disk height is attributable to two factors—disk degeneration and an increased curvature of the vertebral endplate, often from osteoporotic changes in the vertebral cancellous bone (91). There is also a significant trend toward increasing midbody transverse diameter of the lumbar vertebrae with age, amounting to 14% between the ages of 20 to 80 years in men (91).

In considering other age changes in the mature spine, one should distinguish between the relatively minor changes that represent natural aging, more significant atrophic changes

associated with inactivity, and more significant changes associated with disease. In general, when changes in overall mobility are associated with natural aging, they first become evident in the most challenging of physical activities (226). As an example, although 50% of young adult men are willing to lift a 500-N weight, only 15% of men aged between 60 and 65 years may be willing to do so (62).

In regard to age changes at the organ level, it is well known that the strength of bone is proportional to its mineral density. In general, trabecular bone density starts to decrease in the fourth decade, with losses of up to 30% being observed in elderly men and up to 50% in elderly women (151). When a loss in bone density does occur with age, the lumbar vertebrae have been demonstrated to be susceptible to compression failures (37,50). In men, for example, when average vertebral bone density has decreased to 105 mg/ml as measured using quantitative computer tomography, there is a 25% risk of a vertebral fracture, whereas at 45 mg/ml the fracture risk rises to 99% (215). In women, the risk of a vertebral fracture rises 2.2-fold or more for every standard deviation loss in bone mass in postmenopausal women, whether it is measured using dual-photon absorptiometry or quantitative computer tomography (73). Expressed another way, a postmenopausal woman with a bone mineral content that is two standard deviations below the mean value for her age has a 20% risk of spine fracture during the next 3.6 years (73). Osteoporotic fractures lead to an average reduction in anterior and midvertebral height of 25% (99); because the posterior height of the vertebra remains unchanged, this reduction will usually cause a local increase in kyphosis. As far as the functional consequences of osteoporosis are concerned, women with osteoporotic fractures of the spine have been shown to be three times more likely to have difficulty with activities of daily living such as descending stairs, lifting, bending, and walking (104), presumably from activity-related discomfort and/or pain.

Spinal ligaments, as typified by the anterior and posterior longitudinal ligaments, undergo changes of 7%, 28%, and 22%, in elasticity, residual deformation, and energy dissipation, respectively, between the second and seventh decades (269).

It is not uncommon for muscle strength to decrease with advancing age. For example, an approximately 30% loss in isometric strength in the trunk extensors and flexors has been noted between the fourth and eighth decades of life, with the most rapid loss occurring after 50 years of age (60,281). Much of this strength loss can likely be explained by the 30% loss in trunk muscle cross-sectional areas in muscles such as the psoas major and erector spinae over a similar time span (120). We have also found a 30% to 40% loss in the rate of developing isometric strength with age, which appears to be linked to a change in muscle contractility (265). If this finding in the ankle muscles is also found valid in the trunk muscles, it would mean that the rapid deceleration or acceleration of the trunk relative to the pelvis in emergent situations such as a fall would become increasingly challenging with age.

Even in frail elderly, striated muscle retains its ability to gain strength with training, and, depending on the baseline value, strength increases of up to 100% have been recorded in as little as 10 weeks (96). The fact that increases in elderly muscle strength of 20% to 60% were associated with increases in muscle cross-sectional area of approximately 20% (214) suggests that at least some of this increase may be related to improved coordination and/or cognitive factors.

Degeneration

Disk degeneration is usually graded *in vivo* using qualitative radiographic measures of osteophytes and loss of disk height. More recently, magnetic resonance imaging offers a method for quantifying the loss of hydration within the disk (290). Macroscopic disk degeneration *in vitro* is graded by visual inspection and classified according to one of four grades according to Nachemson's scheme (174). Degeneration starts in the second decade

of life and continues steadily thereafter (Fig. 6). The gradual yellowing of the disk that occurs with age is apparently contributed by modification of proteins linked to the collagen (115). Loss of nuclear material is characteristic of degeneration. An experimental study has shown that the disk and its intradiscal pressure are sensitive to loss of nuclear material: loss of just 1 g of nuclear tissue results in a disk height loss of about 0.8 mm and an increase in annular bulge of 0.2 mm (54). The risk for disk degeneration has been shown to be increased in the presence of facet tropism (asymmetry) (188).

Does degeneration affect spine mechanical properties? In one study, Nachemson and coworkers (181) found no effect of degeneration on lumbar vertebral behavior. In another, larger study, Koeller and colleagues (131) also found little effect of age on compression stiffness but did find an increase in creep in elderly spines. So, at present, it appears that degeneration in itself does not lead to dramatic changes in disk mechanical properties. Although increased lumbar laxity at low loads, chiefly in the so-called "neutral zone," has recently been reported in degenerated disks (200), these results are unlikely to be of much significance because compressive preloads of a magnitude similar to those acting *in vivo* are already known to stiffen such disks (123). With the advent of osteophytes, however, one can expect stiffness to increase by a factor of two (167).

The Relationship of Mechanical Factors to Some Clinical Conditions

Spondylolysis and Spondylolisthesis

Spondylolysis refers to a defect in the pars interarticularis, which may be dysplastic, and results in elongation, thinning, and eventual breakage of this structure. A number of theories have been proposed for the pathogenesis of spondylolysis, including heredity and fatigue failures. Certainly, a higher prevalence of spondylolysis has been demonstrated among relatives of patients with this condition (296). Spondylolysis is rarely observed before the age of 5. Its incidence increases

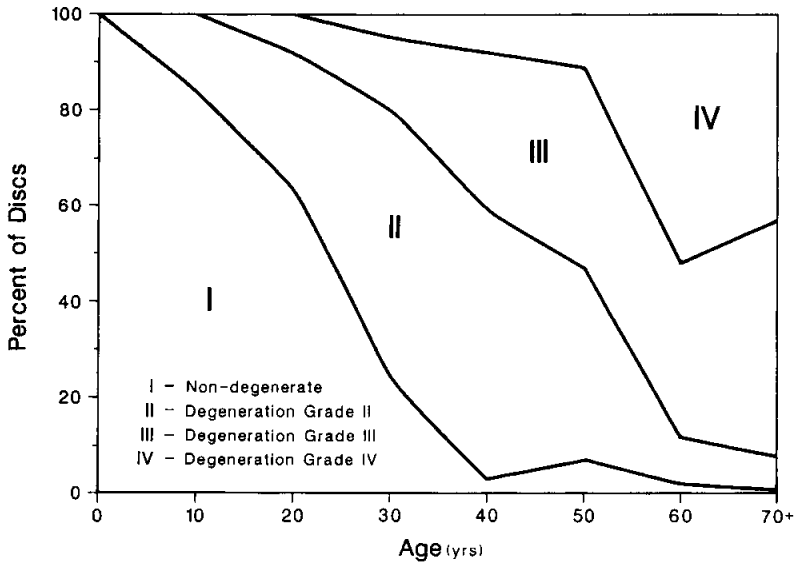

FIG. 6. Percentage of intervertebral disks in each degeneration grade by age. Grade I disks are nondegenerate, whereas grade IV disks are severely degenerate, as defined by Nachemson (174). Data are for 600 disks (19).

from 4.4% in 6-year-old children to 5.8% in adults (98). Certain athletic activities are known to be associated with significant increases in the risk of developing spondylolysis. For example, a fourfold increase in the prevalence of spondylolysis has been observed in female adolescent gymnasts; this rate (i.e., 20.7%) was similar to that found in male high school and university athletes (116,121). Cricket fast bowlers are also at risk for developing spondylolysis: this activity involves repeated near-maximal accelerations and asymmetric motions of the trunk from a position of extension into axial twisting and anterolateral bending on the run (97). The caudal spine level seems to be particularly predisposed to spondylolysis: in one series of 255 patients, 226 (88.6%) had spondylolysis occurring at the L5–Sl level; in the remainder it occurred at the L4–5 level (219).

What mechanical factors are involved? Troup (272) and Cyron and Hutton (75) proposed that repeated extension of the spine, particularly when combined with compression loading, can lead to a fatigue fracture of the pars interarticularis. If the intensity, duration, or rate of the activity increases sufficiently to produce bony microfractures in the pars interarticularis that accumulate faster than can be repaired, a fatigue fracture seems to be a reasonable mode of failure. At present, conclusive proof of this pathogenesis is not available.

Spondylolisthesis is the slippage of one vertebra on another. Usually this results from a defect in the pars interarticularis, a defect in the pedicle, an elongation of the pars and pedicle, or degeneration of the disk. Again, this usually occurs at the L5–S1 level. Degenerative spondylolisthesis at the L4–5 level has been associated with sagittal orientation of the facet joints (105).

Segmental Hypermobility Versus Spine Instability

Much confusion exists in the orthopaedic and spine biomechanics literature concerning the term "spine instability." This is a term that is poorly defined and often misused (21). In mechanical terms, an unstable structure is one in which a small load causes a large (sometimes catastrophic) increase in displacement. Another way of describing this behavior is to say that the structure has experienced a drastic loss of stiffness. A fracture or tumor can cause such behavior. But spines that are classified clinically as having "instability" just because their segmental motions are a few millimeters or degrees more than normal do not exhibit signs of mechanical instability. In regard to these issues, Ashton-Miller and Schultz have argued:

> that the spine is seldom mechanically unstable, rather for many cases that are discussed clinically, it is spine segment hypermobility that is the relevant concept. Decreased spine segment stiffness, evidenced by larger-than-normal vertebral motions on standardized radiographs, should be termed "segmental hypermobility" not "segmental instability" or "spinal instability." Indeed, the measurement of "motion" by itself, without also measuring the associated applied loads (forces and/or moments) that induce the motion, is not fully meaningful, because observed motions always depend on applied loads and loads that produce those motions are seldom quantified, especially *in vivo*. We suggest ways to standardize spine loads when evaluations of segmental hypermobility are to be made. Finally, the definition and measurement of spine segmental hypermobility should be independent of (a) its possible causes (e.g., disk degeneration) and (b) its possible consequences (e.g., neurological deficits) (21).

Thus, loads *and* motions, not just motions, are needed to quantify the stiffness, the flexibility, and, therefore, the instability of the spine. Attempts have been made *in vitro* to quantify hypermobility in the cervical spine in terms of such measurements (201).

In summary, the term "spinal instability" should be reserved for a very specific mechanical behavior, most often associated with trauma, very severe osteoarthrosis, tumor, infection, or iatrogenic causes. It should not be used just to describe segmental motions that are modestly larger than normal, nor should it be used to describe symptomatology. If a spine segment does not display catastrophic dis-

placements, defined in one study as exceeding 12° (185), under known standardized loadings typical of daily activities, then it does not exhibit signs of mechanical instability.

Trunk Muscle Strengths

Maximum isometric voluntary strengths of the lumbar trunk muscles have been reported by several groups (161,234,250). The mean moments that healthy young adult males can develop about low lumbar motion segments in an upright standing position are on the order of 200 Nm in attempted trunk extension, 150 Nm in attempted trunk flexion or lateral bending, and 90 Nm in attempted twisting. The strengths of healthy young adult females are approximately 60% of these values.

The passive moment resistances developed by lumbar motion segments in bending or twisting motions of a few degrees are only a few newton-meters (see Lumbar Spine, above). In upright positions, where motion segments are rotated only a small amount, these passive resistances are negligible compared to the moments that can be actively developed by the trunk muscles. However, when substantially rotated, lumbar motion segments can develop passive moment resistances on the order of 60 Nm (23). In configurations involving substantial bending or twisting of the spine, passive bending resistances are no longer negligible.

While maximum isometric strengths faithfully reflect the strength available to perform tasks slowly, they may not always reflect the strength available during tasks requiring rapid movements because of the well-known Hill hyperbolic relationship describing the reduction of muscle contractile force with increasing muscle fiber shortening velocity. Recognizing this, several investigators have reported lifting strengths and lumbar trunk muscle strengths in tasks in which the trunk is moved at constant angular rates (130,186). Smith and collaborators (250), however, found that when the trunk is moved at rates up to 120°/sec, lumbar trunk strengths are quite similar to strengths measured isometrically. A review of trunk isokinetic strength test results has appeared (187).

Moroney and co-workers (167) measured the maximum voluntary isometric strength of neck muscles. In healthy, young adult subjects, mean strength was on the order of 26 Nm in attempted neck extension, 10 Nm in attempted flexion, 13 Nm in attempted lateral bending, and 9 Nm in attempted twisting. Thus, neck muscle voluntary strengths are an order of magnitude smaller than lumbar trunk muscle strengths.

As mentioned already, muscle properties are significantly affected by aging. After age 30 years, for example, isometric muscle strength is known to decrease by from 18% to 40% by age 65 years (for example, see review by Chaffin and Ashton-Miller [60]).

Myoelectric Measurements

The loads imposed on spine motion segments and the muscle contraction forces developed in physical task performances cannot be measured directly *in vivo.* However, they can be quantified indirectly by measurements of intradiscal pressures (see Disk Pressures, below) and measurements of myoelectric signals. The latter arise because motor nerves engender muscle contractions through the transmission of electrical signals. Such signals are called myoelectric activities. Semiquantitative measurements of spine myoelectric activities have been reported by many groups, including Walters and Partridge (286) in the anterior abdominal muscles, Carlsöo (59) in an array of trunk muscles, Morris and colleagues (169), Pauly (203), Donisch and Basmajian (83) in the back muscles, and Ashton-Miller and colleagues in studying cervical muscle response to acute pain (16).

Quantitative measurements of trunk muscle activities have been reported by Andersson and colleagues (11), Schultz and colleagues (236), and Pope and colleagues (210). Such measurements have demonstrated that the recruitment patterns of trunk muscles vary in a repeatable manner at a given spine level when the direction of an external moment is changed in a sys-

tematic manner (137). Myoelectric signals are noisy, and their absolute values are affected by many variables that cannot easily be controlled. However, when signals are averaged over subject populations and compared on a relative basis from task to task, they can more readily be interpreted quantitatively. The papers last cited used these ideas to interpret the measured activities. A chief use of such measurements is for the validation of biomechanical model analyses (see Rigid-Body Models, below) of muscle contraction forces.

Disk Pressures

Nachemson (174) demonstrated that the pressure developed within the nucleus pulposus of a nondegenerated cadaver lumbar intervertebral disk is nearly proportional to the compressive load on the motion segment containing that disk. This intradiscal pressure is approximately 1.5 times the compression load divided by the transverse cross-sectional area of the disk. Schultz and colleagues (237) showed that other modes of loading seldom modify this proportionality substantially. Thus, measurements of intradiscal pressure provide a means to estimate spine compression loads. Even in cadaveric motion segments, intradiscal pressure has been shown to increase by 100% from the erect posture to the fully forward flexed posture, partly as a result of tension generated in the posterior intervertebral ligaments in such postures (1). Such increases in intradiscal pressure cause the vertebral endplate to deflect into the vertebral body (53) and, when combined with additional compressive loads, can even cause failure of the endplate (114).

Nachemson and Morris (177) used intradiscal pressures to determine *in vivo* compression loads on the lumbar spine resulting from task performances. Subsequent studies have been reported or reviewed by Nachemson and Elfström (175), Andersson and coworkers (12), Nachemson (178), and Schultz and colleagues (230). Pressures within the nucleus of the L-3 disk are typically 300 kPa in relaxed upright standing configurations, corresponding roughly to a compression equal to the weight of the body segments superior to L-3, and more than four times this value in relatively modest exertions. A chief use of intradiscal pressure measurements has been the validation of biomechanical model predictions (see Rigid-Body Models, below) of spine loads.

Trunk Cavity Pressurization

It was recognized as early as 1900 that trunk cavity pressurization is sometimes used to relieve loads on the spine (9). Davis (78), Bartelink (29), and Morris and collaborators (170) contributed some of the earlier reports of abdominal cavity pressure measurements during physical task performances. Typically, during a heavy exertion, abdominal cavity pressure peaks are on the order of 13.3 kPa (100 mm Hg), and Eie and Wehn (88) found cavity pressures in a weight lifter as high as 26.7 kPa (200 mm Hg). Morris and colleagues (170) reported thoracic cavity pressure measurements as well and analyzed the load-relieving effects of such pressures.

Scaled anatomic cross sections show that the area of the abdominal cavity is on the order of 50% of the product of lumbar trunk width times depth, or approximately 300 cm^2 in an average-size male adult (92). A cavity pressure of 13.3 kPa then yields a resultant force of approximately 400 N. The cavity cross-section centroid lies anterior to the intervertebral disk center at a distance that is approximately 42% of trunk depth, or about 8.4 cm. So, large abdominal cavity pressures can produce flexion-relieving moments about a lumbar intervertebral disk center on the order of 34 Nm. This is particularly true when the transversus abdominis, rather than the rectus abdominis muscle, is the abdominal wall muscle most highly correlated with abdominal cavity pressure (68).

Measurements of abdominal cavity pressures during task performances have been proposed as indicators of spine load (79,147).

However, some evidence indicates that this may not be an accurate measure (230,271), and whether abdominal cavity pressurization actually reduces loads on the spine has been questioned (180). One might speculate that a possible role for the increased abdominal wall muscle activity and simultaneously raised intraabdominal pressure during heavy exertions may be to help stiffen the spine and trunk (267).

BIOMECHANICAL MODEL ANALYSIS

Rigid-Body Models to Determine Trunk Loads

Studies that seek to examine the role of mechanical factors in low-back pain epidemiology or to design industrial work schemes to reduce worker back muscle fatigue, for example, require knowledge of the loads placed on the trunk structures when a physical task is performed. The easiest and safest route to that knowledge is biomechanical model analysis. Tasks that are performed slowly can be modeled effectively using concepts of rigid-body equilibrium, and those performed rapidly are examined more appropriately using concepts of rigid-body dynamics. Morris and co-workers (170) were among the first to attempt a biomechanical analysis of quasistatic trunk loads. King (129) reviewed many of the biomechanical model analyses that have been reported in the literature on the musculoskeletal system. The relevant ideas will be illustrated through calculations of lumbar trunk internal loads, but similar ideas can be used to calculate internal loads on any musculoskeletal system structures. The following section illustrates the use of one modeling approach.

Cross-Section Muscle Models

Animals move and exert forces on their surroundings through the use of their muscles. Cross-sectional muscle models, based on concepts of rigid-body equilibrium, allow analyses to be made of effects produced by muscular contraction. This section illustrates analyses that determine the external loads that can be resisted or developed when lumbar trunk muscles are contracted with known tensions. The following sections illustrate the converse; that is, they show what sets of muscle tensions are required to resist or develop a known external load. The former analyses are relatively simple; the latter are often more complicated.

Figure 7 shows a model of ten single-equivalent muscles through a transverse section of the lumbar trunk at the L-3 level (236). Note that a horizontal plane through L-3 does not intersect bony structures other than those of the spine. This is a convenient reference plane because analysis of load transmission paths through multiple bony structures may be quite complex. Table 5 details representative values of the areas, centroidal locations, and lines of action of those muscles. Similar data have been gathered by others (157,184). Table 6 presents the equations of equilibrium that describe the net force and moment developed by these muscles about the center of the L-3 intervertebral disk. Solutions of these equations serve to predict how a physical task performance will load the structures of the trunk. These equations incorporate the assumption that the lumbar motion segment can resist compression and shear forces but not significant bending moments. This is because, although the passive bending resistance developed by a lumbar motion segment in small rotations is only a few newton-meters per degree, net moments are often on the order of 100 Nm.

Calculation of Net Reactions from Given Contraction Forces: Estimates of Isometric Trunk Strengths

The muscle cross-section model just described, or similar models, can be used to estimate maximum isometric trunk strengths. When muscles are contracted with known forces, the model equations can be used to compute the resulting net reaction force. The